Journal of Statistical Physics, Vol. 100, Nos. 1/2, 2000

Overlapping Associating Fluids with Directional Bonds in a Bulk and Near a Hard Wall: Monte Carlo Study

Douglas Henderson,[1] Ian Garcia,[2] Stefan Sokołowski,[3] and Andrij Trokhymchuk[1, 4, 5]

Received July 23, 1999; final February 15, 2000

Two models have been used in these Monte Carlo simulations: the original model with an angular-dependent associative interaction and a model with an angular-averaged potential, which is better suited for simulation and computationaly more efficient. We show that in the homogeneous case under the same conditions, both models yield a nearly identical interparticle structure, but with a slightly different degree of dimerization. This causes differences between these models in the local density distribution of monomers and dimers when an inhomogeneity is present, though the resulting local total density distribution is found to be the same. The theoretical predictions based on Wertheim's theory of association are always closer to the simulation data for the model with the angular-averaged potential.

KEY WORDS: Associating fluids; directional bonding; structure; local density distribution.

1. INTRODUCTION

It is a pleasure to dedicate this paper to George Stell. George has produced an extensive body of important results, much of which has benefited us in

[1] Department of Chemistry and Biochemistry, Brigham Young University, Provo, Utah 84602.

[2] Direccion General de Servicios de Computo Academico, UNAM, Coyoacán, 04510, México D.F.

[3] Department for the Modelling of Physico-Chemical Processes, Faculty of Chemistry, MCS University, 20031 Lublin, Poland.

[4] Instituto de Química, UNAM, Coyoacán, 04510, México D.F.

[5] Permanent address: Institute for Condensed Matter Physics, National Academy of Sciences of the Ukraine, 290011 Lviv, Ukraine.

0022-4715/00/0700-0153$18.00/0

our research. In addition, George's infectious good humor has enlivened many meetings. On this happy occaison, we wish George well in his future scientific and personal life.

Homogeneous molecular association is the one of the areas of statistical-mechanics theory of condensed matter where George has contributed considerably. In the present note we will use some of his ideas to study the associating fluids under confinement. The presence of confinement generates a nonuniformity in the system that influences the degree of molecular association and could significantly affect the physical and chemical properties of a fluid.

The statistical-mechanics treatment of associating fluids is additionally complicated, in comparision with simple fluids, due to the increased number of internal degrees of freedom and coupled intra- and intermolecular interactions between associating atoms. The problem of understanding the behaviour of associating fluids at a fundamental level can be divided into two steps, i.e., the development of suitable models and their adequate description. A number of so-called "primitive" models of associating fluids have been proposed and discussed recently [e.g. see refs. 1–3]. All of them, according to Kalyuzhnyi and Stell[4], fall into two basic types: those with a spherically symmetric attraction and those with an angular-dependent attraction. Among the models belonging to the first type the best studied is the spherically symmetric dimerizing shell model of Stell and Cummings[5]. This model qualitatively reproduces the behaviour of real inhomogeneous associating fluids but is limited to rather short dimer bond lengths, i.e., not more than a half of particle diameter. The more suitable are site-site models in which the associating interaction is due to off-center atom sites, leading to directional atom-atom bonding practically of any desired length l. The simplest among this type of models is a one-component fluid of N dimerizing hard spheres interacting via the potential[6]

$$U(\mathbf{12}) = U_{\text{non}}(\mathbf{12}) + U_{\text{as}}(\mathbf{12}) \tag{1}$$

where **1** and **2** denote the position $\mathbf{r}_1, \mathbf{r}_2$ of the particles 1 and 2. $U_{\text{non}}(\mathbf{12})$ is the nonassociative part of the potential

$$U_{\text{non}}(\mathbf{12}) = U_{\text{non}}(r_{12}) = \begin{cases} \infty, & r_{12} < l \\ D, & l < r_{12} < \sigma \\ 0, & r_{12} > \sigma \end{cases} \tag{2}$$

and

$$U_{\text{as}}(\mathbf{12}) = U_{\text{as}}(x_{12}) = \begin{cases} -\varepsilon, & x_{12} \leqslant a \\ 0, & x_{12} > a \end{cases} \tag{3}$$

is the part of the potential that is responsible for the association. Here $x_{12} = |\mathbf{r}_{12} + \mathbf{d}(\Omega_1) - \mathbf{d}(\Omega_2)|$, $\mathbf{d}(\Omega)$ denotes the position and orientation of the attractive interaction site embedded into the hard core, σ, defined by the nonassociative interactions; ε and a are the strength and the range of associative attraction, respectively; D is the height of the square mound, satisfying the condition: $\exp[-\beta D] \simeq 0$, where $\beta = 1/kT$; l is the bonding length. The geometric parameters of the interaction are subject to the restriction $l < 2d + a < l + (2 - \sqrt{3})\, d$, to ensure steric saturation at the dimer level[6].

The theoretical description of this model uses a two-density formalism, i.e., it introduces the densities of bonded [dimerized], ρ_1, and unbonded [monomer], ρ_0, particles. The integral equation approach is based on the solution of Wertheim Ornstein–Zernike (WOZ) equation[6] under the associative Percus–Yevick (APY) approximation[1]. We label this approach as the WOZ/APY theory. The most important ingredient that is necessary in Wertheim's theory is the associative "Mayer function," $f_{\text{as}}(r)$. This characterizes the bonding effects and is defined as[6]:

$$
\begin{aligned}
f_{\text{as}}(r_{12}) &= \int d\Omega_1 \int d\Omega_2 \exp[-\beta U_{\text{non}}(r_{12})]\{\exp[-\beta U_{\text{as}}(x_{12})] - 1\} \\
&= \exp[-\beta U_{\text{as}}(r_{12})] \qquad (4) \\
&= \begin{cases} \dfrac{(2a - 2d + r_{12})(a + 2d - r_{12})^2}{24\, d^2 r_{12}}\, e^{\beta\varepsilon}, & L < r_{12} < 2d + a \\ 0, & \text{otherwise} \end{cases}
\end{aligned}
$$

From Eq. (4) it can be seen that the original angular-dependent associative potential $U_{\text{as}}(x_{12})$ [we will refer to it as model M1] is replaced by an effective "angular-averaged" potential $U_{\text{as}}(r_{12})$ [we will refer to it as model M2], i.e., the set of WOZ/APY equations is usually solved for a model M2 that may differ from the original one. The geometrical constraints, defining number of possible bonds, however, remain unchanged: they are satisfied implicitly by the structure of the WOZ equation.

The aim of present study is to address the following two questions: (i) how different are *the overlapping dimerizing fluids* modelled via the original angular-dependent potential (3) and the via effective angular-averaged potential (4) and (ii) how good are the theories, based on the angular-averaged potential (4) in the prediction of the dimerizing fluid properties compared with computer simulations performed for the both potential models.

2. MONTE CARLO SIMULATIONS

In order to answer these questions, we have performed two series of canonical ensemble MC simulations. In the first series, which we call homogeneous, we obtain the total radial distribution functions (RDFs), $g(r)$, and the degree of dimerization, $\lambda = \rho_1/\rho$, of the bulk fluid where $\rho = \rho_0 + \rho_1$ is the total particle number density, N/V. In the second, inhomogeneous, series we extracted information about the local density distributions (LDDs) of the monomer, $\rho_0(z)$, and dimerized, $\rho_1(z)$, species of the fluid near a hard wall. Both series of simulations have been performed for two potential models of hard-core spheres of diameter σ, i.e., M1 defined by potential (3) and M2 corresponded to angular-averaged potential introduced in (4). To define the model M2 we used in the Metropolis Monte Carlo (MC) algorithm[7] for the exponent of the associative interaction, $\exp[-\beta U_{as}(r_{12})]$, the expression written in the second row of Eq. (4) supplemented by the restriction that each particle can form only one associative bond. The last requirement has been introduced in the MC algorithm in order to make model M2 consistent with the steric constraints imposed by the original model M1.

The simulation cell for homogeneous simulation was a cubic box with a length $L = 10\sigma$ on each edge, while in the inhomogeneous case it was rectangular with the same xy base and a length $H = 12\sigma$ in the z direction that was large enough to avoid any interference between the two hard walls located at $z = 0$ and $z = H$; it also provides us to with a reasonable homogeneous region in the middle of the simulation cell during inhomogeneous simulations. Periodic boundary conditions, with box length L, were imposed in the all three directions during the homogeneous simulations and in the x and y directions in the inhomogeneous case. The particle-wall interaction was modelled by hard-sphere/hard-wall type potential.

An initial configuration for each simulation run has been chosen by the random placing of N hard-sphere particles in a simulation cell. Each particle has a bonding site with a random orientation. During the simulation, a trial move consisting of a translational displacement and reorientation was applied to each particle in turn. As in the case of association via a spherically symmetrical shell, two sizes of translational displacement were used[1]: a small one of order of the range of associative interaction, a, and a large one of order of particle diameter, σ. In the case of the model M1, in addition to the trial move of a single particle, we have introduced trial moves that translate and rotate entire dimers in random directions. This makes the sampling of the configurational space in the simulations of dimerizing fluids more efficient. Such an additional type of trial move is not necessary when model M2 is applied. The parameters of the translational

and orientational moves have been chosen to assure an overall acceptance ratio of the order of 25 to 50 per cent.

Ensemble averages were accumulated over $N \times 10^6$ configurations after equilibrating from a random distribution for $N \times 10^6$ configurations in the case of model M1, and $N \times 10^5$ configurations in the case of model M2. The resulting RDFs and LDDs were evaluated from histograms updated every $2N$ configurations with a grid size of $0 \cdot 01\sigma$. For the intraparticle part of RDFs $[r < \sigma]$ the grid size was reduced to $0 \cdot 001\sigma$ to obtain more insight into the details of dimer formation. In addition to the LDDs of the centers of mass of all the particles, $\rho(z) = \rho_0(z) + \rho_1(z)$, we have calculated the LDDs of the centers of mass of the formed dimers, $\rho_{CD}(z)$, and the angular distributions of dimers or density-orientation profiles of dimers, $\rho_D(z, t)$, where $t = \cos\theta$, and θ is the tilting angle of the dimer axis with respect to the normal to the wall. The grid size for t was $0 \cdot 05$. All simulation runs have been performed using an Origin 2000 supercomputer with 32 nodes located at UNAM.

3. RESULTS AND DISCUSSIONS

From a practical point of view, the most interesting case is when the particle-particle bonding length, l, is large but still shorter than the center-to-center distance, i.e., the dimerizing species overlap, changing the excluded volume of the system. In the present study the following set of parameters of the associative interactions, given by Eqs. (3) and (4), have been chosen: $l = 0.9$, $d = 0.45$, $a = 0.1$. All are given in units of the hard-sphere diameter, $\sigma = 1$, which is taken as the length unit throughout the paper. In all our calculations presented here, we have used two fixed values of the reduced strength of associative interactions, namely, $\beta\varepsilon = 7$ and 12.

The scheme of our calculation is as follows. We first performed MC simulations for the inhomogeneous case to define the corresponding total bulk density, $\rho^B = \rho_0^B + \rho_1^B$, i.e., the homogeneous density in the middle region of the simulation cell. The number of particles in the inhomogeneous simulations were chosen to be $N = 500$ and 900. The resulting bulk densities for both models are collected in Table 1. The first important observation is that for all simulation runs with the same number of particles, N, despite the differences in the bulk number densities of the monomers, ρ_0^B, and dimers, ρ_1^B, the total bulk densities, ρ^B, are practically the same for both models. Thus, for the homogeneous calculations we define two densities, namely, $\rho = 0.4$ and 0.705. For each of these densities we have performed independent series of homogeneous MC simulations for both model as well as theoretical calculations through the WOZ/APY theory[1, 6].

Table 1. MC Results for the Bulk (B) Densities from Inhomogeneous Simulations for the Model with Angle-Dependent Associative Potential (Model M1) and for the Model with "Angle-Averaged" Associative Interaction (Model M2)[a]

	N	$\beta\varepsilon$	ρ^B	ρ_0^B	ρ_1^B	λ^B
Model M1	500	7	0.4015 ± 0.0022	0.3457 ± 0.0022	0.0558 ± 0.0008	0.1390 ± 0.0021
Model M2	500	7	0.4020 ± 0.0025	0.3517 ± 0.0025	0.0502 ± 0.0004	0.1249 ± 0.0013
Model M1	500	12	0.4041 ± 0.0022	0.1480 ± 0.0015	0.2561 ± 0.0014	0.6337 ± 0.0027
Model M2	500	12	0.4059 ± 0.0017	0.0747 ± 0.0008	0.3312 ± 0.0012	0.8158 ± 0.0016
Model M1	900	7	0.7111 ± 0.0058	0.4720 ± 0.0088	0.2391 ± 0.0095	0.3361 ± 0.0124
Model M2	900	7	0.7116 ± 0.0082	0.4920 ± 0.0067	0.2196 ± 0.0023	0.3085 ± 0.0026
Model M1	900	12	0.7120 ± 0.0054	0.1578 ± 0.0115	0.5541 ± 0.0127	0.7782 ± 0.0163
Model M2	900	12	0.7130 ± 0.0034	0.0712 ± 0.0018	0.6418 ± 0.0033	0.9001 ± 0.0025

[a] The uncertainties represent one standard deviation during the MC production runs.

To avoid locked metastable configurations[8] during the simulation runs and to be sure of the efficiency of the space sampling[9], we have controlled the uniformity of the density distributions of monomers and dimers in the simulation cell along x, y, and z directions for all four homogeneous simulation runs. We found that all curves are flat within a small error bar,

Table 2. WOZ/APY Theory Predictions and MC Results for the Partial Densities and Degree of Dimerization of a Homogeneous Overlapping Dimerizing Fluid[a]

	$\beta\varepsilon$	ρ	ρ_0	ρ_1	λ
MC/M1			0.3533	0.0467 ± 0.0003	0.1167 ± 0.0008 (0.1183)
MC/M2	7	0.4	0.3509	0.0491 ± 0.0001	0.1228 ± 0.0001 (0.1228)
WOZ/APY			0.3526	0.0474	0.1185
MC/M1			0.1470	0.2530 ± 0.0004	0.6326 ± 0.0011 (0.6351)
MC/M2	12	0.4	0.0752	0.3248 ± 0.0001	0.8121 ± 0.0001 (0.8123)
WOZ/APY			0.0770	0.3130	0.8075
MC/M1			0.4953	0.2097 ± 0.0009	0.2975 ± 0.0013 (0.2984)
MC/M2	7	0.705	0.4914	0.2136 ± 0.0001	0.3029 ± 0.0001 (0.3031)
WOZ/APY			0.5159	0.1891	0.2682
MC/M1			0.1589	0.5461 ± 0.0008	0.7746 ± 0.0011 (0.7756)
MC/M2	12	0.705	0.0722	0.6328 ± 0.0001	0.8975 ± 0.0001 (0.8975)
WOZ/APY			0.0795	0.6255	0.8872

[a] The uncertainties represent one standard deviation during the MC production runs.

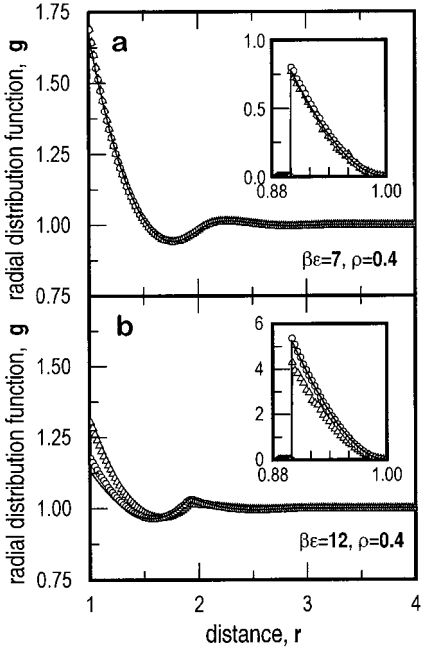

Fig. 1. A comparison of the total RDF, $g(r)$, obtained from the WOZ/APY theory (solid thick line) and from the homogeneous MC simulations for model M1 (squares) and model M2 (triangles). The interparticle distance, r, is scaled by hard-core diameter, σ. The main part of the figure and the inset are for the interparticle $[r > \sigma]$ and intraparticle $[r < \sigma]$ parts, respectively. Parts a and b are for $\beta\varepsilon = 7$ and 12, respectively. The number density of particles in the theory and simulation, $\rho = 0.4$.

as is usual in a computer experiment, i.e., all our systems have been in equilibrium and space sampling was quite efficient; no evidence of any metastable configurations has been observed.

The complete results from the homogeneous calculations are collected in Table 2 and plotted in Figs. 1 and 2. Examining the MC data from the Tables 1 and 2, we note a high degree of coincidence of the bulk monomer and dimer densities resulting from an independent series of homogeneous and inhomogeneous simulations. Also from Table 2 we see that the degree of dimerization, λ, predicted by the WOZ/APY theory, acording to the self-consistency relation[6]

$$\lambda + 4\pi\rho(1-\lambda)^2 \int f_{\text{as}}(r)\, y_{00}(r)\, dr = 0 \tag{5}$$

falls into the range between those for the two simulation models, being always a little lower than results of model M2 and notably differ from

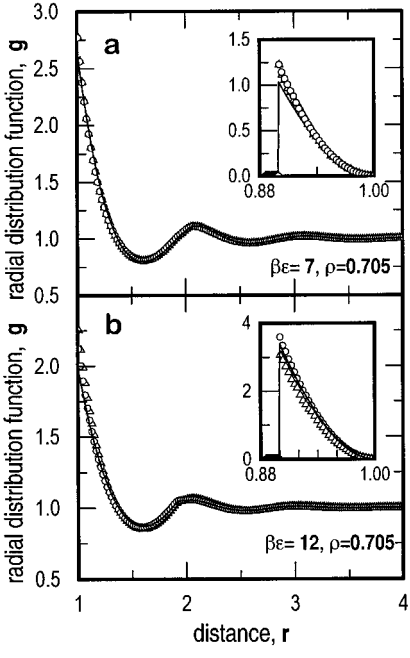

Fig. 2. The same as in Fig. 1, but for the particle number density, $\rho = 0.705$.

Table 3. MC Results for the Wall (W) Densities of an Inhomogeneous Overlapping Dimerizing Fluid[a]

	$\beta\varepsilon$	ρ^B	ρ^W	ρ_0^W	ρ_1^W	λ^W
MC/M1		0.4015 ± 0.0022	0.9632	0.8879	0.0755	0.0784
MC/M2	7	0.4020 ± 0.0025	0.9690	0.8922	0.0770	0.0795
MC/M1		0.4041 ± 0.0022	0.7958	0.3998	0.3968	0.4986
MC/M2	12	0.4059 ± 0.0017	0.7222	0.1947	0.5279	0.7309
MC/M1		0.7111 ± 0.0058	3.7917	2.8294	0.9660	0.2547
MC/M2	7	0.7116 ± 0.0082	3.8647	2.9703	0.8982	0.2324
MC/M1		0.7120 ± 0.0054	3.3015	0.9269	2.3768	0.7199
MC/M2	12	0.7130 ± 0.0034	3.1877	0.4370	2.7523	0.8634

[a] The MC data were obtained from a linear curve fit of histograms near the wall. The uncertainties represent one standard deviation during i the MC production runs.

those of model M1, especially for stronger associative interaction [$y_{00}(r)$ in Eq. (5) is the partial cavity distribution function[6]]. The degree of dimerization in MC simulation has been calculated according to its definition, i.e., $\lambda = \rho_1/\rho$ by counting the average number of bonded particles during production run. For both considered densities, i.e., $\rho = 0.4$ [Fig. 1] and 0.705 [Fig. 2], we can observe a smoothing of the interparticle [$r > \sigma$] parts of $g(r)$ and a lowering of its contact values [$r = \sigma^+$] with an increase of the strength of associative interactions. The second maxima shifts in the direction of smaller interparticle separations and changes its shape [a characteristic cusp, connected with dimer formation appears]. When the associative interaction is weaker [parts (a) of Figs. 1 and 2], the agreement of the interparticle parts of $g(r)$ that are obtained from the MC simulations for both models as well as from the theory, is quite good. With an increase of the strength of associative interaction, the differences between the simulation results for models M1 and M2 increase. Model M1 always gives

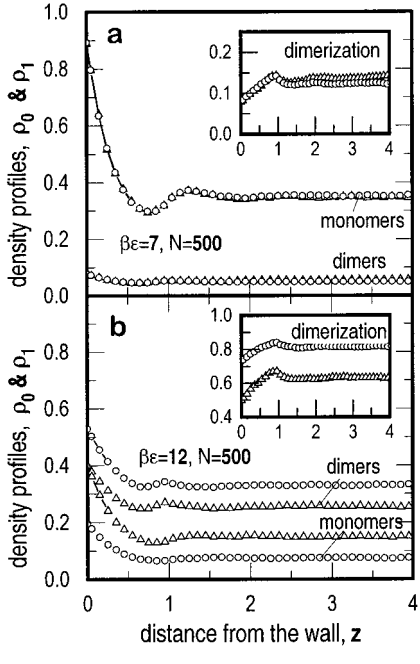

Fig. 3. The MC local density distribution of monomers, $\rho_0(z)$, and dimerized particles, $\rho_1(z)$, (the main part of the figure) and the degree of dimerization, $\lambda(z)$, (the inset) for model M1 (dashed line) and model M2 (solid line). The particle-wall distance, z, is scaled by hard-core diameter, σ. Parts a and b are for $\beta\varepsilon = 7$ and 12, respectively. The number of particles in simulation, $N = 500$.

the highest contact value $g(r=\sigma^+)$. Moreover, increasing differences in the magnitude and the location of the first minima and second maxima of $g(r)$ between model M1 and M2 are observed. Model M2 always gives a smoother function $g(r)$ that is due to the higher degree of dimerization of this model. At both densities, the WOZ/APY theory results show a clear tendency to be closer to the simulation results for model M2. The intraparticle $[r>\sigma]$ parts of $g(r)$, evaluated from the simulations, indicate nonnegliglible differences in the magnitude of the intraparticle associative maxima between the models M1 and M2: the magnitude of the intraparticle peak in model M1 is always lower than for M2. The intraparticle parts of $g(r)$, evaluated from the WOZ/APY theory, have a height and the shape that are very close to those evaluated from the simulations for model M2. This is consistent with lower degree of dimerization, λ, for model M1, which in simulations also can be calculated by integrating the intraparticle part of $g(r)$,

$$\lambda = 4\pi\rho \int_0^{\sigma} g(r)\, r^2\, dr. \tag{6}$$

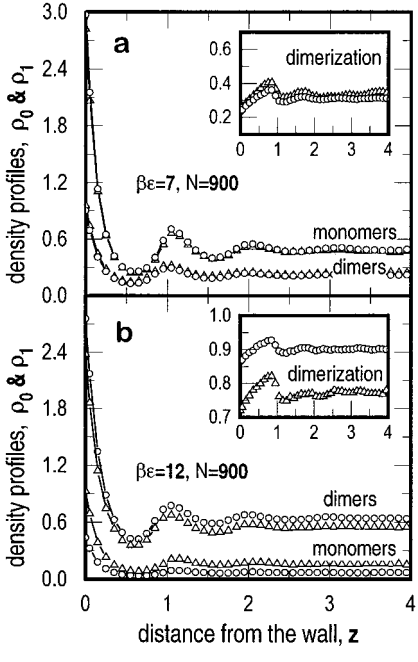

Fig. 4. The same as in Fig. 3, but for the number of particles in simulation, $N=900$.

The data, calculated according to Eq. (6), are shown in Table 2 in parenthesis. The definitions of the degree of dimerization in the simulations are not exactly the same as that of Wertheim. However, the simulation and WOZ/APY results for λ are nearly the same, indicating that this method of calculating λ in the simulations is for all practical purposes equivalent to the WOZ/APY definition.

The discussed differences for the intraparticle part of RDFs, i.e., differences in the bulk monomer and dimer densities for the two models M1 and M2, cause some differences between them when the LDDs near a hard wall are analyzed (Table 3). In Figs. 3 and 4 we show the LDD profiles of the monomers, $\rho_0(z)$, dimers, $\rho_1(z)$, and the degree of dimerization, $\lambda(z)$, obtained for both models. The major difference in the local density distribution between two models is observed at stronger associative interaction. In this case, all curves for both models have a similar shape but are shifted in magnitude for some value [perhaps this is the reason for

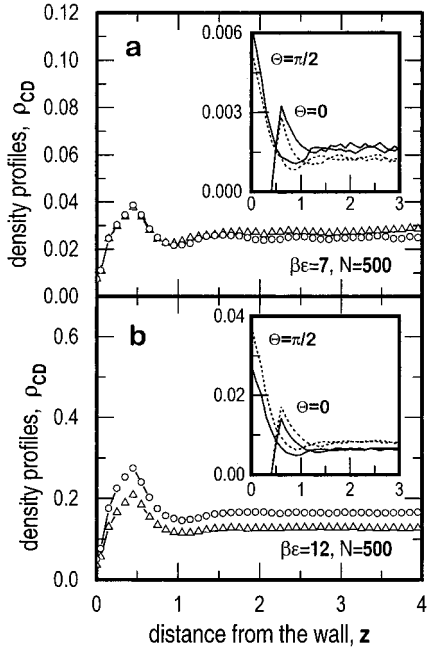

Fig. 5. The MC local density distribution of the dimer's center of mass, $\rho_{CD}(z)$, (the main part of the figure) and radial slices through the density-orientation profile of the dimers, $\rho_D(z, t)$, (the inset) for model M1 (dashed line) and model M2 (solid line). The particle-wall distance, z, is scaled by hard-core diameter, σ. Parts a and b are for $\beta\varepsilon = 7$ and 12, respectively. The number of particles in the simulation, $N = 500$.

the scaling of the interaction parameter when a comparison of angular-dependent simulation data with thermodynamic perturbation theory (TPT) or density functional theory is performed]. Both models lead to the same conclusion that, at least for the parameters considered in present study, the local density of dimerized particles at the wall is always higher than in the bulk, though the degree of dimerization in the bulk region is higher than in the first wall layer. This is due to the high adsorption of the monomer species. At the same time the fraction of monomers always is lower in the second layer where the degree of dimerization has an absolute maxima.

The local orientational ordering for both models is quite similar, as can be seen from Figs. 5 and 6, where the LDDs of the dimer's center of mass and local density-orientation profiles of the dimers that are oriented parallel, $\rho_D(z, t=0)$, and perpendicular, $\rho_D(z, t=1)$, to the wall, are shown: the parallel orientation of the dimers is favored. An increasing density of dimers in the vicinity of the wall leads to more dimers becoming oriented parallel to the wall and the extension of this orientational distribution to the second and third layer is observed.

We note that despite the fact that some differences in the local *partial* density distributions of monomers and dimers for both models (see Figs. 3

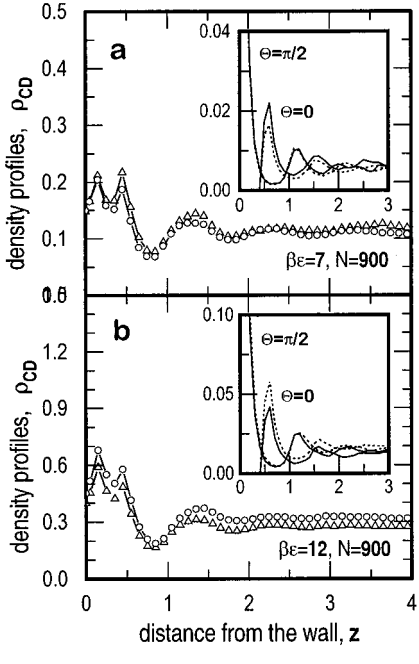

Fig. 6. The same as in Fig. 5, but for the number of the particles in simulation, $N=900$.

and 4) are observed, the local *total* density profiles, $\rho(z) = \rho_0(z) + \rho_1(z)$, are practicaly identical, except in the close vicinity of the wall, i.e., $z = 0$. The difference between $\rho(z = 0)$ for model M1 and M2 is the consequence of the difference in the degrees of dimerization for both models in the homogeneous phase [see Table 2], i.e., the difference in the bulk thermodynamics [pressure, compressibility *etc.*], since the value of total density $\rho(0)$, according to the contact value theorem[10], gives the bulk gas pressure, P/kT.

4. CONCLUSIONS

Summarizing, we have analyzed the model used in Wertheim's theory of association and found that it may be different from the original one that usually is used in MC simulations. We have performed canonical MC simulations for both models in a bulk phase and near a hard wall. The main descrepancies between two models in a homogeneous phase are the resulting different degree of dimerization, i.e., under the same conditions the fraction of formed dimers in each model is different. A comparison of the theory with the homogeneous MC simulation data indicates that the WOZ/APY equations accurately predicts the structure and composition of overlapping dimerizing fluids when a comparison is performed for the same Hamiltonian. We would like to stress that our tests of the accuracy of the bulk structure predicted by the integral equation theory, are methodologically different from those performed in the literature[11–13], where thermodynamic properties have been calculated. Firstly, in refs. (11–13) the associative site was located outside the core of the interacting spheres; this seems to be an important difference. Secondly, to reproduce thermodynamic properties, TPT was used to evaluate the degree of dimerization by fitting, in a certain meaning, the theory to the simulation data. The integral equation approach used in this work is self-consistent in this sense.

The differencies in degree of dimerization for both models will cause different homogeneous thermodynamics. When inhomogeneity is included, this is reflected in the different total density distribution in the vicinity of the hard wall that is in accordance with the contact value theorem.

Obviously, one can expect increasing differences between models M1 and M2, when more than one associative site is embedded into the core. Nevertheless, model M2 introduced here seems to have several advantages. First, it is spherically symmetric and thus much simpler and significantly less computationally demanding in MC studies. Secondly, it is consistent with the Wertheim's theory. Moreover, even in the case of multiple

associative sites, it may be useful to find a more accurate definition of the "angular-averaged" associative potential. Thus, we can expect that the model M2 will be applied in future studies of associating fluids.

ACKNOWLEDGMENTS

This work was partially supported by CONACYT of Mexico (Grant No 25301-E). D.H. is grateful for the financial support of the National Science Foundation (Grants No CHE96-01971 and CHE98-13729) and the donors of the Petroleum Research Fund, administered by the American Chemical Society (Grant No ACS-PRF 31573-AC9). S.S. is grateful to KBN for financial support of this work (Grant No. 3T0909A6210). A.T. is grateful to Brigham Young University for its hospitality during his stay in Provo.

REFERENCES

1. Yu. V. Kalyuzhnyi, G. Stell, M. L. Llano-Restrepo, W. G. Chapman, and M. F. Holovko, *J. Chem. Phys.* **101**:7939 (1994).
2. W. R. Smith and I. Nezbeda, *J. Chem. Phys.* **81**:3694 (1984).
3. I. Nezbeda and J. Slovak, *Mol. Phys.* **90**:353 (1997).
4. Yu. V. Kalyuzhnyi and G. Stell, *Mol. Phys.* **78**:1247 (1993).
5. P. T. Cummings and G. Stell, *Mol. Phys.* **51**:253 (1984).
6. M. S. Wertheim, *J. Stat. Phys.* **35**:19; 35 (1984); **42**:459;477 (1986).
7. N. A. Metropolis, A. W. Rosenbluth, M. N. Rosenbluth, A. H. Teller, and E. Teller, *J. Chem. Phys.* **21**:1087 (1953).
8. C. J. Segura and W. G. Chapman, *Mol. Phys.* **86**:415 (1995).
9. N. A. Busch, M. S. Wertheim, Y. C. Chiew, and M. L. Yarmush, *J. Chem. Phys.* **101**:3147 (1994).
10. I. Nezbeda, M. R. Reddy, and W. R. Smith, *Mol. Phys.* **71**:915 (1990).
11. C. G. Joslin, C. G. Gray, W. G. Chapman, and K. E. Gubbins, *Mol. Phys.* **62**:843 (1987).
12. G. Jackson, W. G. Chapman, and K. E. Gubbins, *Mol. Phys.* **65**:1 (1988).
13. W. G. Chapman, *Mol. Phys.* **93**:4299 (1990).